

Article

Adsorption Behavior and Adsorption Dynamics of Micrometer-Sized Polymer Microspheres on the Surface of Quartz Sand

Jun Li ¹, Taotao Luo ^{1,*}, Wende Yan ¹, Tingting Cheng ¹, Keyang Cheng ¹, Lu Yu ², Jiannan Cao ¹ and Zhongquan Yang ¹ 

¹ Institute of Petroleum and Natural Gas Engineering, Chongqing University of Science and Technology, Chongqing 401331, China; 2011927@cqust.edu.cn (J.L.)

² Exploration and Development Research Institute of Southwest Branch, SINOPEC, Chengdu 610041, China

* Correspondence: 2017039@cqust.edu.cn

Abstract: The adsorption of polymer microspheres in a stratum can directly affect its action mode and performance in the actual application process. Understanding the adsorption pattern of polymer microspheres and their adsorption mechanism can facilitate optimization of the application mode and enhance the use efficiency. Ultraviolet spectrophotometry was employed to measure the static adsorption characteristics of polymer microspheres (PMS) on the surface of quartz sand. The PMS adsorption capacity on the surface of quartz sand increased with increasing concentration. When the concentration was 1000 mg/L, the static equilibrium adsorption capacity was 402 µg/g, and monolayer adsorption was dominant. The effect of the contact time on the adsorption was investigated, and the fitting was performed using the isothermal adsorption thermodynamic equilibrium model and the adsorption kinetic model. The adsorption of 800 mg/L PMS tended to equilibrate after 0.8 h of adsorption on the surface of quartz sand, and the adsorption of 1400 mg/L PMS tended to equilibrate after 1 h of adsorption on the surface of quartz sand. Good fitting results of the kinetic adsorption process were obtained using the pseudo-first-order (PFO) model, pseudo-second-order (PSO) model, Elovich model, and mixed-order (MO) model. The effects of the temperature, particle size of the quartz sand, solid–liquid ratio, and salinity on the adsorption of PMS on the surface of quartz sand were examined. The PMS adsorption capacity on the surface of quartz sand decreased with increasing environmental temperature. The adsorption of PMS at the solid–liquid interface was an exothermic process, and the enthalpy of adsorption was negative. As the mass of the quartz sand in the solid–liquid ratio increased, the adsorption capacity decreased; a low salinity and neutral pH were conducive to the adsorption of PMS on the surface of quartz sand.

Keywords: polymer microspheres; static adsorption; isothermal adsorption thermodynamic equilibrium model; adsorption kinetic model; adsorption pattern



Citation: Li, J.; Luo, T.; Yan, W.; Cheng, T.; Cheng, K.; Yu, L.; Cao, J.; Yang, Z. Adsorption Behavior and Adsorption Dynamics of Micrometer-Sized Polymer Microspheres on the Surface of Quartz Sand. *Processes* **2023**, *11*, 1432. <https://doi.org/10.3390/pr11051432>

Academic Editor: Federica Raganati

Received: 2 April 2023

Revised: 13 April 2023

Accepted: 28 April 2023

Published: 8 May 2023



Copyright: © 2023 by the authors. Licensee MDPI, Basel, Switzerland. This article is an open access article distributed under the terms and conditions of the Creative Commons Attribution (CC BY) license (<https://creativecommons.org/licenses/by/4.0/>).

1. Introduction

For oilfields developed via water flooding, the water cut value of most wells increases with increasing well production time [1]. This is because, under long-term water flooding, the deposits in the stratum are gradually washed away. Large pore throats are formed in the reservoir, and the permeability increases, exhibiting the characteristics of heterogeneous reservoirs [2]. The subsequent injected water will continue to advance along the high-permeability layer and cannot effectively spread to the remaining oil area, so the reservoir cannot be efficiently exploited. To solve this problem, researchers began to focus on the theory and technique of adjusting the water injection profile in the deep layer of the oil reservoir. Polymer microspheres (PMS) are a novel plugging agent with a rapid development and wide application scope. PMS are spherical gel particles and have good water-absorbing and swelling properties. After swelling, their volume can increase from

several folds to several dozen folds. In addition, since the initial size of PMS is smaller than the reservoir pore throat size, PMS can be transported to the deep layer of the reservoir. After absorbing water and swelling, relying on the retention, jamming, bridging, and sealing effects, blockage of the pore throats occurs [3], and the high permeability formation is plugged off so that the injected fluid produces an effective diversion, the sweep coefficient of the displacement agent is enhanced, and the production rate is improved.

When a fluid comes into contact with a solid, one or more components in the fluid accumulate on the surface of the solid, which is called adsorption. Adsorption also refers to the phenomenon of a substance (mainly a solid substance) with surface-absorbing molecules or ions from the surrounding medium (liquid or gas) [4]. Adsorption is a mass transfer process where molecules inside a substance and surrounding molecules have a gravitational attraction to each other, but molecules on the surface of the substance do not fully exert the external forces relative to the substance [5]. Therefore, the surface of a liquid or solid substance can adsorb other liquids or gases, especially when the surface area is large. This adsorption force can have a significant effect, so large areas of substances are often used in industry for adsorption, such as activated carbon, water film, gas, etc. Zhou et al. [6] have studied methane adsorption mechanisms on Longmaxi shale and demonstrated that methane should be not only adsorbed in micropores (<2 nm) but also in mesopores (2–50 nm) by two hypotheses. Haitao Wang et al. [7] have proposed a mathematical model describing the transient pressure behaviors of a vertical well with MRHF in a stress-sensitive CBM reservoir; the adsorption–desorption and diffusion for fluid in reservoirs are considered. Xi Zhang et al. [8] have investigated the effect of ammonium sulfate on the adsorption characteristics of low-concentration Pb(II) ions on the sulfidized hemimorphite surface and showed that ammonium sulfate could increase the maximum recovery of hemimorphite from 69.42% to 88.24% under low concentration of Pb(II) ions. Zuhao Kou et al. [9] have established a model to determine bottom-hole pressure during CO₂ injection through a hydraulic fractured multiwell-pad, considering CO₂ viscous flow, diffusion, and adsorption in shale reservoirs.

PMS have adjusting and driving functions, and their seepage process in porous media is relatively complex, involving the interaction relationship between PMS and the rocks in the reservoir. The adsorption characteristics of PMS on the surface of quartz sand need to be explored. In this study, polymer microsphere (PMS) were synthesized by suspension polymerization, and the water absorption expansion performance of PMS in deionized water and salt water was evaluated. These studies will be beneficial for analyzing the migration and sealing performance of polymer microspheres in porous media.

2. Experimental Details

2.1. Experimental Materials and Equipment

2.1.1. Experimental Materials

The inverse suspension polymerization technique is one of the methods used to prepare PMS. In this method, only a small amount of surfactant needs to be added as a dispersant to ensure that the water phase is dispersed in the oil phase and the monomers are polymerized in the water phase [10]. The inverse suspension polymerization technique has the advantages of uniform polymerization, a fast reaction rate, a high yield of solution polymerization, and a simple process [11]. Additionally, in the polymerization process, the reaction system has a low apparent viscosity and good stability. In this study, the starting materials used to prepare the PMS using the inverse suspension polymerization included a monomer, crosslinking agent, and initiator. The main reagents are shown in Table 1.

Table 1. Reagents used in the experiment.

	Name	Purity	Manufacturer
Reactive monomer	Acrylamide (AM)	Chemically pure	Tianjin Fucheng Chemical Reagent Factory, Tianjin, China
	2-Acrylamide-2-methylpropanesulfonic acid (AMPS)	Chemically pure	Tianjin Fucheng Chemical Reagent Factory, Tianjin, China
	Hydrophobic monomer	Purity > 80%	Self-prepared
Crosslinking agent	N,N'-methylenebisacrylamide	>98%	Chengdu Kelong Chemical Reagent Factory, Chengdu, China
Initiator	Potassium persulfate	Analytical reagent (AR)	Chengdu Kelong Chemical Reagent Factory, Chengdu, China
	Sodium sulfite	AR	Chengdu Kelong Chemical Reagent Factory, Chengdu, China
	Edetate disodium	AR	Chengdu Kelong Chemical Reagent Factory, Chengdu, China
	Quartz sand	20~30 mesh	Chengdu Kelong Chemical Reagent Factory, Chengdu, China

2.1.2. Instruments

After the PMS were prepared, the particle size distribution after the PMS absorbed water and swelled was characterized, and the ultraviolet (UV) spectrophotometry method was adopted to measure the concentration of the polymer microspheres. The instruments used are described in Table 2.

Table 2. Instruments used in the experiment.

	Instrument Name	Instrument Model	Manufacturer
Instruments for reaction	Heat-gathering constant temperature heating magnetic stirrer	DF-101S	Zhengzhou Greatwall Scientific Industrial and Trade Co., Ltd., Zhengzhou, China
	pH meter	FE20	Mettler-Toledo Instruments (Shanghai), Ltd., Shanghai, China
	Mixer	IKA	IKA-Werke GmbH & Co. KG, Staufen im Breisgau, Germany
Instruments for characterization	Electric constant temperature blast drying oven	DHG-9140A	Beijing Luxi Technology Co., Ltd., Beijing, China
	Particle Size Analyzer	Mastersizer 3000	Malvern Panalytical Ltd., Malvern, UK
	Dual-beam scanning UV-vis spectrophotometer	T9	Beijing Persee General Instrument Co., Ltd., Beijing, China
	Digital ultrasonic cleaner	KH3200DE	Kunshan Hechuang Ultrasonic Instrument Co., Ltd., Kunshan, China

2.1.3. Experiment Methodology

A Malvern Panalytical Mastersizer 3000 made by UK was used to measure the microsphere size and particle size distribution of the PMS.

Using UV spectrophotometry, the concentration and content of the substances were measured based on the Lambert–Beer law. Due to the different structures of substances, they can have absorption spectra at specific wavelengths, and the absorbance is directly proportional to the concentration. Using the strong absorption peak of amide groups in polyacrylamide at around 200 nm, Xiao et al. [12] found that there was an excellent linear relationship between the polyacrylamide concentration and UV absorbance when the polyacrylamide concentration was lower than 250 mg/L, and there were few interferences from factors such as the salinity and temperature. PMS are obtained from the polymerization of monomers, such as acrylamide, and have amide groups similar to polyacrylamide. Liu et al. [13] used UV spectrophotometry to measure the content of polymer microspheres in a solution, determined the optimal absorption wavelength of the experiment and the measurement range of the effective concentration, and calculated the concentration of the polymer microspheres in the solution according to the linear regression equation.

2.2. Experimental Contents and Steps

2.2.1. Preparation of Polymer Microspheres

Water phase: The reactive monomers, i.e., acrylamide (AM), 2-acrylamide-2-methylpropanesulfonic acid (AMPS), and N,N'-methylenebisacrylamide, were added to deionized water according to a certain ratio, and the mixture was stirred continuously. When all of the solids were dissolved, the pH of the solution was adjusted to neutral using sodium hydroxide. Subsequently, the hydrophobic monomer was added, followed by the addition of a small amount of surfactant to allow the hydrophobic monomer to be dispersed in the water. Finally, a small amount of edetate disodium was added to form the reactive water phase.

Oil phase: Certain amounts of surfactants Span80 and Tween-80 were dissolved in #3 white oil as dispersion liquids, and the reactive oil phase was formed after stirring.

Initiator: Potassium persulfate and sodium sulfite were dissolved in a small amount of deionized water for future use.

Inverse suspension polymerization process: First, the reactive oil phase was added to a three-neck flask. The reactive water phase was added to a pressure-equalizing graduated addition funnel, and then it was added dropwise to the reactive water phase while the reactive oil phase was stirred at a low speed, and oxygen was expelled by introducing nitrogen. During the dropwise addition of the reactive water phase, an initiator was added to the reaction system using a syringe. Then, the temperature was raised to the set temperature, and the reaction proceeded under continuous stirring for a certain period of time. After the reaction solution was cooled down, the upper oil phase was removed, absolute ethanol and acetone were added to perform demulsification, and washing and extraction were conducted multiple times. The PMS product was obtained after drying in an oven at 80 °C. The reaction process is shown in Figure 1.

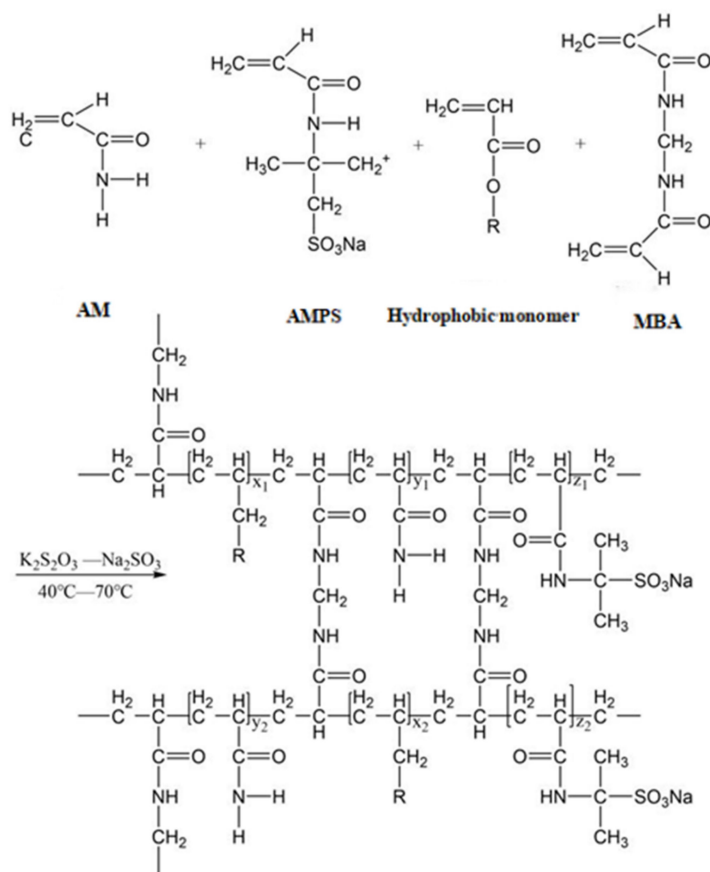


Figure 1. Reaction flowchart of PMS.

2.2.2. Particle Size Distribution Characteristics of PMS

The PMS were placed and dispersed in the deionized water to form a suspension, the initial particle size was measured, and the change in the particle size was measured after the PMS swelled completely (60 h). The simulated water of one oilfield formation with a total salinity of 14,695.89 mg/L was used as the salt solution. The PMS were placed in the simulated salt solution to swell completely (60 h), and the change in the particle size was measured.

2.2.3. Measurement of the Amount of Adsorbed PMS

(1) Plotting the standard curve

Standard aqueous solutions with concentrations of 100 mg/L and 200 mg/L were prepared, and a UV spectrophotometer was used to conduct full-range scanning. The absorption spectra are shown in Figure 2. The PMS exhibited a peak absorbance at 202 nm, and, therefore, 202 nm was selected as the wavelength to measure the PMS.

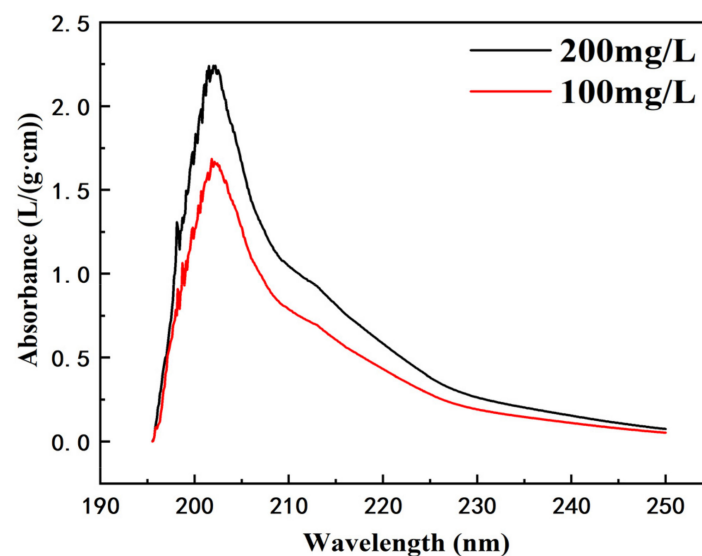


Figure 2. Ultraviolet Absorption Spectrogram of PMS.

The 50–1000 mg/L PMS standard solutions were prepared in deionized water and saline water, with a concentration gradient difference of 100 mg/L. With 202 nm as the fixed absorption wavelength, the absorbance of the various standard concentrations was measured.

(2) Calculation of the amount of adsorbed PMS

In the calculation of the amount of adsorbed PMS, the adsorption of the PMS on the wall during the liquid transfer was ignored. Using the difference in the PMS concentration before and after the adsorption and the amount of added quartz sand, the amount of PMS adsorbed by the quartz sand was calculated.

$$\Gamma = \frac{(C_0 - C)V}{\omega} \quad (1)$$

where C_0 and C are the initial concentrations of the polymer particles and the sample concentration after adsorption (mg/L), respectively; V is the volume of the PMS solution added (mL); ω is the mass of quartz sand added (g); and Γ is the amount of adsorbed PMS ($\mu\text{g/g}$).

The schematic diagram of the experimental structure of this paper is shown in Figure 3.

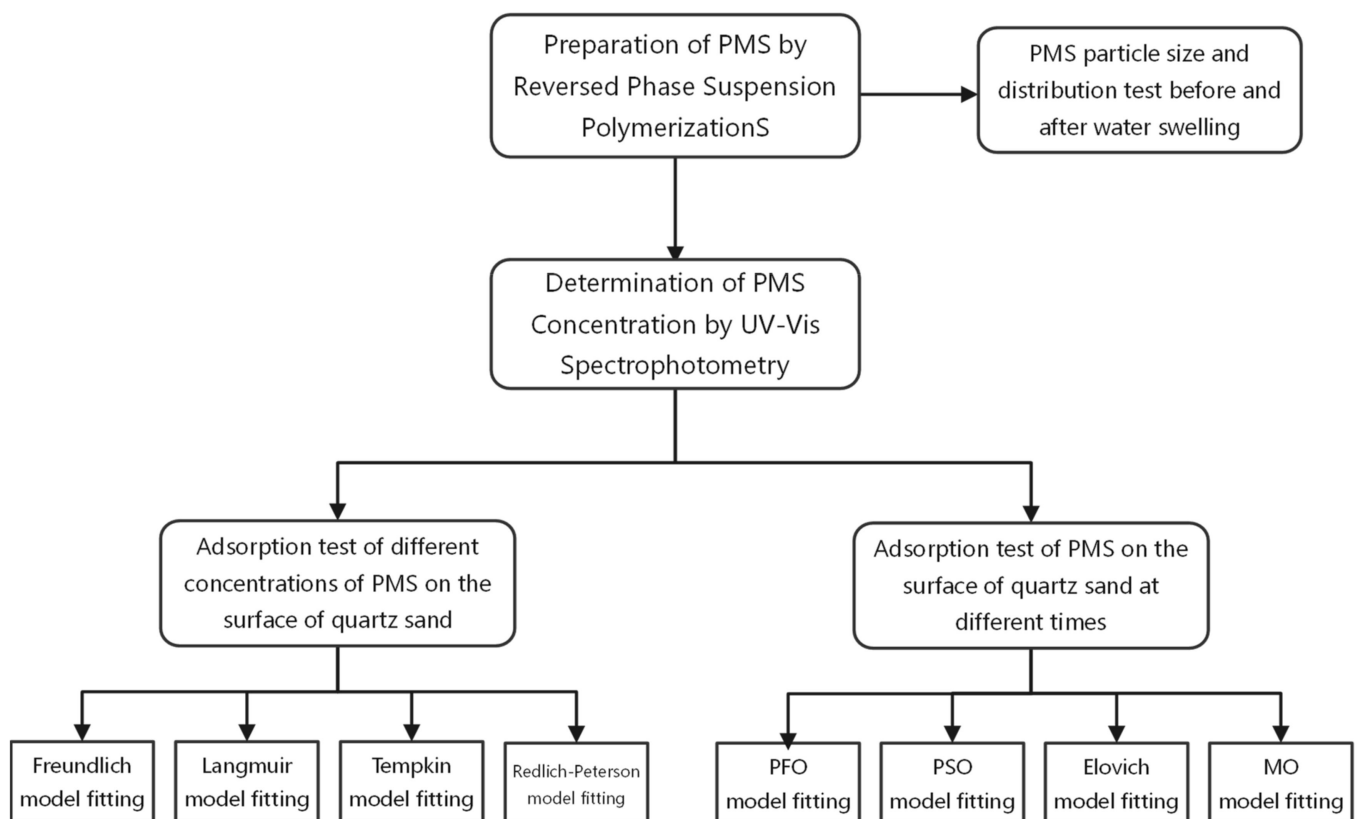


Figure 3. The Structure of all the conducted experiments.

3. Results and Discussion

3.1. Particle Size Distribution Characteristics of PMS

The initial particle size of the PMS, the particle size of the PMS after complete swelling in deionized water, and the particle size of the PMS after complete swelling in saline water are shown in Figure 4.

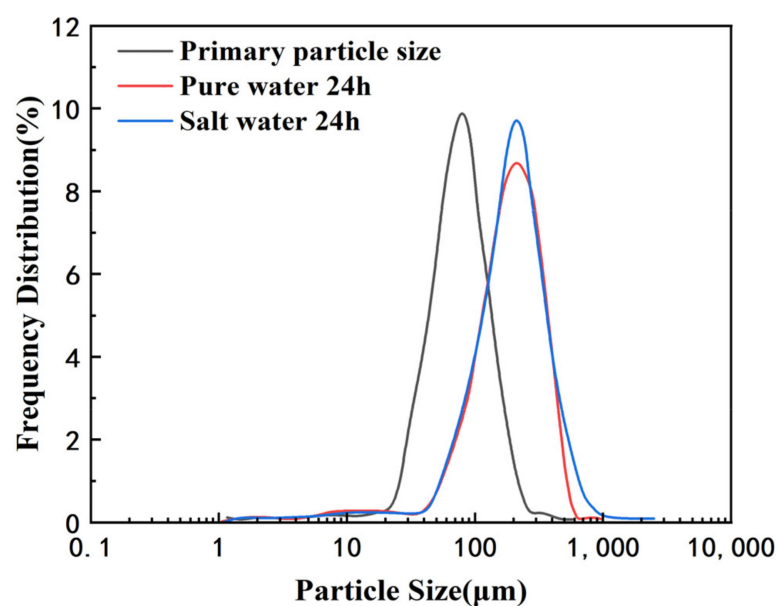


Figure 4. Particle size distribution of PMS before and after swelling.

The experimental results indicate that the PMS exhibited a unimodal normal distribution in water, and the initial average particle size D_{50} was 72 μm . After swelling in the deionized water and saline water for 60 h, the particle size of the PMS increased, and they still exhibited a unimodal normal distribution, but the distribution was wider. The average particle sizes of the PMS after swelling in the deionized water and saline water were 203 μm and 184 μm , respectively. The water entering the PMS was a gradual infiltration process. When the PMS were placed in water, the hydration of the amide and sodium sulfonate in the PMS was favorable for the stretching of the external polymer chains of the PMS, so the water was wrapped inside the PMS. Since the water infiltration and the hydration of the hydrophilic molecules inside the PMS facilitated the entrance of the water into the deep site of the PMS, the volume of the PMS gradually increased. The PMS contained a large number of crosslinks, and it was difficult for the water molecules to enter the PMS. After the hydratability of the internal molecules reached equilibrium, the water molecules could not infiltrate into the PMS, and the PMS did not swell anymore. In the saline water, the hydratability of the amide and sodium sulfonate decreased, and the ability of the water molecules to enter the microspheres decreased to a certain extent, so the swelling ability of the PMS decreased to some extent compared to that in deionized water.

3.2. Characteristics of Isothermal Adsorption of PMS on the Surface of Quartz Sand

3.2.1. Static Adsorption of Different Concentrations of PMS

First, a 5000 mg/L stock solution was prepared, and then it was diluted to 100 mg/L, 250 mg/L, 500 mg/L, 750 mg/L, 800 mg/L, 1000 mg/L, 1200 mg/L, 1400 mg/L, 1800 mg/L, 2000 mg/L, and 3000 mg/L polymer solutions. Next, 80 mL of each of the above solutions was added to a wide neck bottle, acid-washed quartz sand was added according to a solid–solution ratio of 1:10, and the mixture was mixed with a temperature heating magnetic stirrer. After sufficient contact for 24 h, the quartz sand was removed via filtration, and the PMS concentration of the filtrate was measured. In the concentration range of 100–3000 mg/L, the amount of PMS adsorbed on the surface of the quartz sand was measured twice in each experiment. The experimental results are presented in Table 3.

Table 3. Static adsorption capacity under different concentration conditions.

Adsorption Capacity (μg/g)	Concentration of Polymer Solution (mg/L)										
	100	250	500	750	800	1000	1200	1400	1800	2000	3000
#1	132	174	248	336	348	406	405	402	405	401	405
#2	124	176	246	328	347	398	406	404	407	403	401
Average	128	175	247	332	347.5	402	405.5	403	406	402	403

The experimental results indicate that, as the concentration of the PMS solution increased, the quantity of adsorbed PMS gradually increased. When the concentration was 1000 mg/L, the adsorption capacity reached equilibrium, the quantity of adsorbed PMS no longer increased, and the static equilibrium adsorption capacity was around 402 $\mu\text{g/g}$.

3.2.2. Isothermal Adsorption Thermodynamic Equilibrium Model

The four isothermal adsorption thermodynamic equilibrium models and specific parameters are described in Table 4 [14]. The monolayer adsorption on the homogeneous sites and the multilayer adsorption can be modeled using the Langmuir and Freundlich adsorptions, respectively, and the two adsorption isotherms both involve two parameters. The Temkin adsorption isotherm is also a two-parameter model that assumes multilayer adsorption. The Redlich–Peterson adsorption isotherm is the mixed form of the Langmuir and Freundlich models and has three parameters. These two models are suitable for homogeneous or heterogeneous adsorption processes. Generally, all of the adsorption models should be examined using the adsorption data to determine.

Table 4. Adsorption isotherm models.

No.	Model	Function Equation	Parameter Definition
1	Langmuir model	$q_e = \frac{q_o K_L C_e}{1 + K_L C_e}$	q_o is the maximum adsorption capacity per unit mass of adsorbent (mg/g); K_L is the Langmuir adsorption constant (L/mg); C_e is the liquid phase equilibrium concentration (mg/L). q_e is the amount of adsorbed adsorbate per unit weight at adsorption equilibrium (mg/g); K_F is the adsorption constant reflecting the adsorption capacity (L/mg); the value of n is associated with the adsorption strength; C_e is the solution concentration at adsorption equilibrium (mg/L).
2	Freundlich model	$q_e = K_F C_e^{1/n}$	K_T is the Tempkin equilibrium binding constant, which reflects the maximum binding energy (L/mg); B is the Tempkin constant related to the heat of adsorption; $B = R_T/b$, where R is the ideal gas constant (8.314 J/mol K), T is the absolute temperature (K), and b is a constant.
3	Tempkin model	$q_e = B \ln KT + B \ln C_e$	K_r is the Redlich–Peterson isotherm constant (L/g); β is an exponent between 0 and 1.
4	Redlich–Peterson model	$q_e = \frac{K_r C_e}{1 + \alpha C_e^\beta}$	

3.2.3. Analysis of the Fitting Results for the Isothermal Adsorption Thermodynamic Equilibrium Models

Using user-defined functions in the Origin software and linear or nonlinear models, the fitting of the adsorption data for the PMS solutions with different concentrations via the Levenberg–Marquardt optimization algorithm was evaluated using the following parameters: the sum of squared errors (SSE), mean squared error (MSE), root mean square error (RMSE), coefficient of determination (R^2), and chi-square value (χ^2).

According to the Langmuir model, Freundlich model, Tempkin model, and Redlich–Peterson model, the fitting of the static adsorption data was performed. The fitting parameters and calculated results are presented in Table 5, and the model distribution curves are shown in Figure 5.

Table 5. Results for parameters of different models.

Model	Parameter Estimation Results			Model Evaluation			
	Parameter	Estimated Value	SSE	MSE	χ^2	RMSE	R^2
Langmuir model	q_o	482.0388	6883.3525	625.7593	25.6762	25.0152	0.9341
	K_L	0.0031					
Freundlich model	K_F	45.8055	18055.254	1641.3868	58.1445	40.5140	0.8272
	$1/n$	0.2916					
Tempkin model	B	95.1639	11103.728	1009.4298	33.4279	31.7715	0.8937
	KT	0.0411					
Redlich–Peterson model	α	0.0031	6883.3696	625.7609	25.6675	25.0152	0.9341
	β	1.0000					
	K_r	1.4944					

As can be seen from the fitting results presented in Table 5 and Figure 5, the parameter β of the Redlich–Peterson model was close to 1 (β is an empirical constant between 0 and 1). This β value of close to 1 indicates that the quartz sand conformed to the Langmuir model, that is, the adsorption on the surface of the quartz sand was monolayer adsorption and the adsorption action on the PMS was almost even. The fitting accuracy of the Temkin model was lower than that of the Langmuir model, indicating that the adsorption of the PMS on the surface of the quartz sand was not multilayer adsorption. The three-parameter Redlich–Peterson model is a mixed form of the Langmuir model and the Freundlich model, and therefore, it could more accurately describe the isothermal adsorption process (R^2 : 0.827–0.934). The Langmuir model has the highest fitting accuracy, indicating that

PMS has only limited adsorption sites on the surface of quartz sand, rather than unlimited adsorption sites.

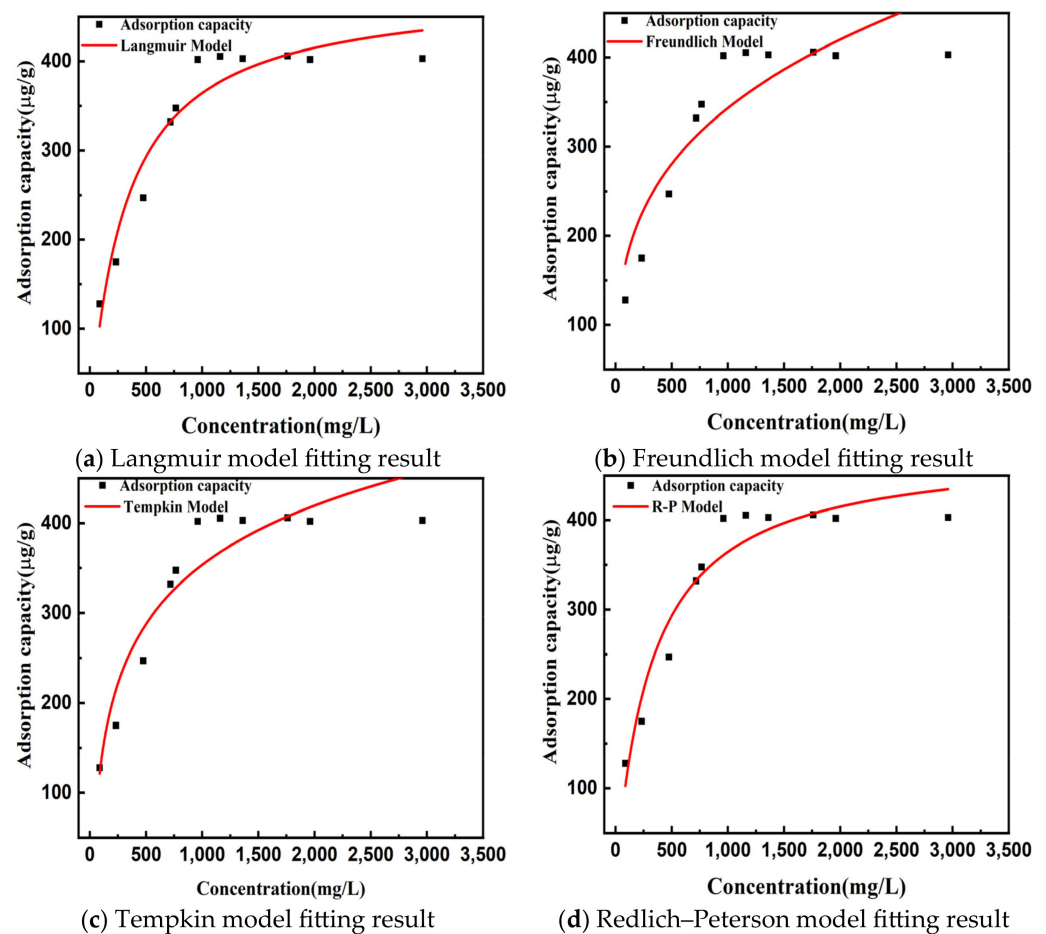


Figure 5. Fitting curves of different models.

3.3. Adsorption Kinetic Characteristics of PMS on the Surface of Quartz Sand

3.3.1. Static Adsorption of PMS with Different Contact Times

First, 800 mg/L and 1400 mg/L PMS solutions were prepared, 80 mL of one of the above solutions was added to a wide neck bottle, quartz sand was added according to a solid–solution ratio of 1:10, and the mixture was mixed by stirring. Sufficient contact was ensured between the polymer solution and the surface of the quartz sand, and the effect of the contact times on the adsorption of the PMS was investigated. The experimental results are shown in Figure 6.

The experimental results shown in Figure 6 reveal that, as the contact time increased, the adsorption of the PMS solution initially increased rapidly and then gradually stabilized. For the 800 mg/L PMS solution, after 0.8 h, the amount of adsorbed PMS reached 345 $\mu\text{g/g}$, and adsorption equilibrium was generally reached. For the 1400 mg/L PMS solution, after 1 h, the amount of adsorbed PMS reached 404 $\mu\text{g/g}$, and adsorption equilibrium was generally reached. This is because there were sufficient adsorption sites on the surface of the quartz sand in the initial stage of adsorption, and the PMS quickly occupied these adsorption sites. Over time, the PMS adsorbed on the surface of the quartz sand gradually accumulated, and the amount of adsorbed PMS increased rapidly. As the adsorption sites on the surface of the quartz sand were gradually occupied, there were fewer and fewer empty sites available for adsorption, and the increase in the amount of PMS adsorbed slowed down until the adsorption reached equilibrium.

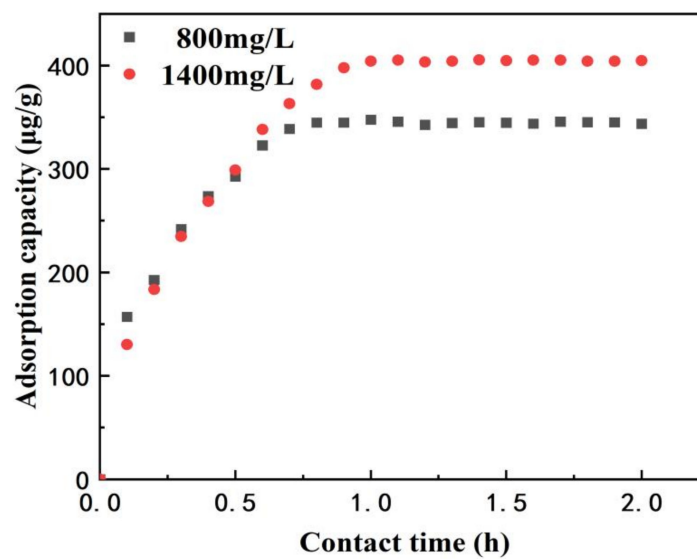


Figure 6. Adsorption of PMS with different concentrations at different contact times.

3.3.2. Kinetic Model of Adsorption Reaction

The kinetics of the adsorption process was mainly studied to describe the solute adsorption rate of the adsorbent. Investigating the adsorption kinetics can provide an understanding of the adsorption and mass transfer process, thus elucidating the adsorption mechanism. The commonly used adsorption kinetic models are the pseudo-first-order (PFO) model [15], pseudo-second-order (PSO) model [16], Elovich model [17], and mixed-order (MO) model [4]. The four adsorption kinetic models and their specific parameters are described in Table 6 [4]. The PFO model is based on the assumption that adsorption is controlled by the diffusion step, and the adsorption rate is proportional to the difference between the equilibrium adsorption capacity and the adsorption capacity at time t . The PSO is based on the assumption that the adsorption rate is limited by the chemisorption mechanism. This chemisorption involves electron sharing and electron transfer between the adsorbents and adsorbates. In addition, the MO is the mixed form of the PFO and PSO. The Elovich equation is an empirical equation that describes the process of a series of reaction mechanisms, such as the diffusion of the solute in the liquid phase or interface and activation and deactivation of the surface. It is very suitable for processes with high activation energy reactions. Furthermore, the Elovich equation can also reveal the irregularity in the data that the other kinetic equations ignore.

Table 6. Adsorption kinetic model.

No.	Model	Function Equation	Parameter Definition
1	PFO model	$\ln(q_e - q_t) = \ln q_e - k_1 t$	q_e and q_t are the amounts of adsorbed adsorbate at adsorption equilibrium and at time t , respectively; k_1 is the adsorption rate coefficient of the quasi-first-order model.
2	PSO model	$\frac{t}{q_t} = \frac{1}{k_2 q_e^2} + \frac{t}{q_e}$	q_e is the adsorption capacity at adsorption equilibrium ($\mu\text{g/g}$); q_t is the adsorption capacity at adsorption time t ($\mu\text{g/g}$); k_2 is the rate constant of the pseudo-second-order reaction ($\text{g/mg}\cdot\text{h}$).
3	Elovich model	$q_t = \frac{1}{b} \ln(ab) + \frac{1}{b} \ln t$	a is the initial adsorption rate constant; b is a parameter related to the degree of surface coverage of the adsorbent and its chemisorption activation energy.
4	MO model	$\frac{dq_t}{dt} = k'_1(q_e - q_t) + k'_2(q_e - q_t)^2$	k'_1 is the first-order rate constant of the mixed-order model (h^{-1}); k'_2 is the second-order rate constant ($\text{g}\cdot\text{mg}^{-1}\cdot\text{h}^{-1}$) of the mixed-order model.

3.3.3. Analysis of the Fitting Results Using the Kinetic Models of the Adsorption Reaction

Using Visual Basic for Application (VBA), a macro language of Visual Basic, the fitting and solving of the different adsorption kinetic models were conducted using linear or nonlinear methods. The parameters used to evaluate the models included the SSE, MSE, RMSE, R^2 , and X^2 . The fitting parameters of each model for the adsorption of the 800 mg/L and 1400 mg/L PMS solutions under different contact times and the calculated results are presented in Table 7, and each model distribution curve is shown in Figure 6.

Table 7. Results for parameters of different models.

Model	Polymer Concentration (mg/L)	Parameter Estimation Results		Model Evaluation				
		Parameter	Estimated Value	SSE	MSE	X^2	RMSE	R^2
PFO model	800	K_1	4.329	2000.401	95.257	12.8530	9.760	0.9877
	1400	K_1	2.927	2042.978	97.285	10.3341	9.863	0.9921
PSO model	800	K_2	0.0168	3162.142	150.578	10.8220	12.271	0.9793
	1400	K_2	0.007	4965.565	236.456	14.4382	15.377	0.9800
Elovich model	800	a	10,250.5	1898.455	90.403	10.3582	9.508	0.9881
		b	0.0156					
	1400	a	3546.51	1907.757	90.846	12.3829	9.531	0.9928
		b	0.010					
MO model	800	K'_1	3.652	1806.366	86.017	9.1183	9.275	0.9883
		K'_2	0.004					
	1400	K'_1	3.098	2599.060	123.765	10.8570	11.125	0.9894
		K'_2	0.000					
		n	0.882					

The fitting results presented in Table 7 and Figure 7 show that the 4 models yielded good fitting results for the adsorption kinetic process. The results for the PFO model and PSO model indicate that the PMS were easily adsorbed on the surface of the quartz sand, and this adsorption action occurred from the beginning of the contact. With increasing contact time, the amount of PMS adsorbed gradually increased, the adsorption equilibrium was reached after 0.8 h and 1 h, respectively, and the adsorption rate was relatively fast. The Elovich model is often used to investigate the existence of a chemisorption process on the nonhomogeneous surface of the adsorbent, and the R^2 value demonstrates that the result of the Elovich model matches the adsorption kinetic process well. The Elovich model shows that the adsorption capacity of PMS on the surface of quartz sand is not uniform, which increases linearly with the increase in PMS coverage on the surface of quartz sand, and the adsorption rate of PMS on the surface of quartz sand is not uniform, which decreases exponentially with the increase in PMS adsorption on the surface of quartz sand. The MO is a mixed form of the PFO and PSO, so its fitting accuracy is relatively high, indicating that the adsorption rate of PMS on the surface of quartz sand is not only proportional to the concentration of PMS in water but also proportional to the square of the concentration of PMS in water.

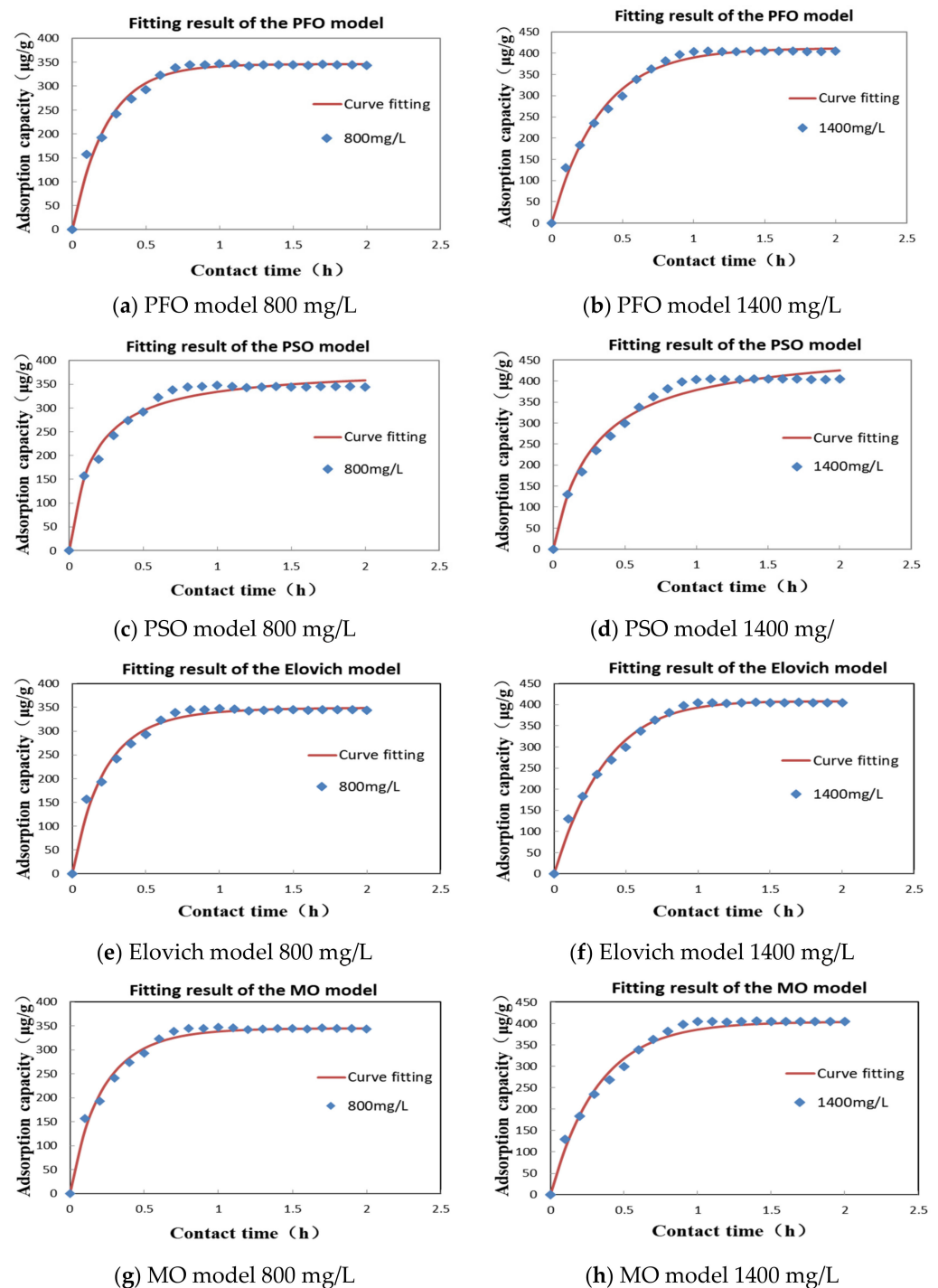


Figure 7. Fitting curves of different models.

4. Conclusions

1. In this study, AM, AMPS, hydrophobic monomer, and crosslinking monomer N,N'-methylene bis acrylamide (MBA) were used as the reactive monomers, and the PMS were prepared using an inverse suspension polymerization. The initial particle size D_{50} was 72 μm , and the average particle sizes after swelling in deionized water and saline water were 203 μm and 184 μm , respectively. Under a fixed UV absorption wavelength of 202 nm, the PMS exhibited a good linear relationship between the concentration and absorbance within the range of 100–500 mg/L.
2. With increasing PMS concentration, the amount of PMS adsorbed on the surface of the quartz sand gradually increased. Studies on the isothermal adsorption behavior

of PMS on the surface of quartz sand shows that the fitting accuracy of the Langmuir model for the isothermal adsorption process was relatively high, indicating that the PMS adsorption on the surface of the quartz sand was dominated by monolayer adsorption and limited adsorption positions.

3. The adsorption kinetics of PMS on the surface of quartz sand shows that good fitting of the adsorption kinetic process was obtained using the PFO model, PSO model, Elovich model, and MO model, and the PFO and PSO models indicate that PMS is easily adsorbed on the surface of quartz sand, and this adsorption has already occurred since the beginning of contact. With the increase in contact time, the adsorption amount gradually increases. The Elovich model shows that the adsorption capacity of PMS on the surface of quartz sand is not uniform. It increases linearly with the increase in PMS coverage on the surface of quartz sand. The adsorption rate of PMS on the surface of quartz sand is not uniform but decreases exponentially with the increase in PMS adsorption on the surface of quartz sand. The mixed (MO) model shows that the adsorption rate of PMS on the surface of quartz sand is not only proportional to the concentration of PMS in water, and the concentration of PMS in water is proportional to the square.

Author Contributions: Conceptualization, J.L., T.L. and T.C.; investigation, W.Y., K.C. and L.Y.; writing—original draft, J.L., T.L. and K.C.; writing—review and editing, J.C. and Z.Y. All authors have read and agreed to the published version of the manuscript.

Funding: This research was funded by the Basic and Frontier Research Programs of Chongqing Science and Technology Commission of China (Grant No. cstc2018jcyjAX0342), This research was funded by the Science and Technology Research Project of the Chongqing Municipal Education Commission of China (grant No. KJQN201901540, No. KJQN201901542, No. KJQN202101). Financial support from the Chongqing Science and Technology Bureau (Grant No. CSTB2022NSCQ-MSX1362, No. sl202100000141, Grant No. CSTB2022BSXM-JCX0152), the Key Laboratory of Ministry of Education of Enhanced Oil and Gas Recovery (Grant No NEPU-EOR-2022-02), and the Science Foundation of Chongqing University of Science and Technology, Chongqing (Grant No. 182101002) is greatly acknowledged.

Data Availability Statement: The data used to support the findings of this study are available from the corresponding author upon request.

Conflicts of Interest: The authors declare no conflict of interest.

References

1. Kang, W.; Zhou, B.; Yang, H.; Li, X.; Zhang, H.; Tang, X.; Gao, Y. Research progress of polymer microspheres for oilfield drive conditioning. *Polym. Mater. Sci. Eng.* **2020**, *36*, 173–180.
2. Wang, S.; Kuai, J.; Song, S.; Ju, Y.; Li, X.; Wang, C. Advances in the study of core-shell polymer microspheres for dissection. *Petrochem. Appl.* **2021**, *40*, 7–10+14.
3. Yang, H.; Kang, W.; Yu, Y.; Yin, X.; Wang, P.; Zhang, X. A new approach to evaluate the particle growth and sedimentation of dispersed polymer microsphere profile control system based on multiple light scattering. *Powder Technol.* **2017**, *315*, 477–485. [\[CrossRef\]](#)
4. Wang, J.; Guo, X. Adsorption kinetic models: Physical meanings, applications, and solving methods. *J. Hazard. Mater.* **2020**, *390*, 122156. [\[CrossRef\]](#) [\[PubMed\]](#)
5. Mozaffari, M.M.; Kermani Vahid, K.; Vahab, G.; Anis, A.; Mika, S. Adsorption isotherm models: A comprehensive and systematic review (2010–2020). *Sci. Total Environ.* **2021**, *812*, 151334. [\[CrossRef\]](#) [\[PubMed\]](#)
6. Zhou, S.; Ning, Y.; Wang, H.; Liu, H.; Xue, H. Investigation of methane adsorption mechanism on Longmaxi shale by combining the micropore filling and monolayer coverage theories. *Adv. Geo-Energy Res.* **2018**, *2*, 269–281. [\[CrossRef\]](#)
7. Wang, H.; Kou, Z.; Guo, J.; Chen, Z. A semi-analytical model for the transient pressure behaviors of a multiple fractured well in a coal seam gas reservoir. *J. Pet. Sci. Eng.* **2021**, *198*, 108159. [\[CrossRef\]](#)
8. Zhang, X.; Deng, J.; Wang, Y.; Li, S.; Zhao, H.; Liu, C.; Ma, Z.; Sun, Z. Adsorption characteristics of Pb (II) ions on sulfidized hemimorphite surface under ammonium sulfate system. *Int. J. Min. Sci. Technol.* **2023**, in press. [\[CrossRef\]](#)
9. Kou, Z.; Zhang, D.; Chen, Z.; Xie, Y. Quantitatively determine CO₂ geosequestration capacity in depleted shale reservoir: A model considering viscous flow, diffusion, and adsorption. *Fuel* **2022**, *309*, 122191. [\[CrossRef\]](#)

10. Yang, H.; Kang, W.; Liu, S.; Bai, B.; Zhao, J.; Zhang, B. Mechanism and influencing factors on the initial particle size and swelling capability of viscoelastic microspheres. *J. Dispers. Sci. Technol.* **2015**, *36*, 1673–1684. [[CrossRef](#)]
11. Yao, C.; Lei, G.; Li, L.; Gao, X. Preparation and characterization of polyacrylamide nanomicrospheres and its profile control and flooding performance. *J. Appl. Polym. Sci.* **2013**, *127*, 3910–3915. [[CrossRef](#)]
12. Xiao, Q. Adsorption performance of polyacrylamide on coal dust. *Drilling Completion Fluids* **2013**, *30*, 46–48+94,95.
13. Liu, Y.; Xu, G.; Ju, Y.; Sun, L.; Zhang, F.; Zhao, W.; Zhnag, K. UV spectrophotometric determination of polymer microsphere output solution concentration. *Sci. Technol. Eng.* **2015**, *15*, 145–149.
14. Kalam, S.; Abu-Khamsin, S.A.; Kamal, M.S.; Patil, S. Surfactant Adsorption Isotherms: A Review. *ACS Omega* **2021**, *6*, 32342–32348. [[CrossRef](#)] [[PubMed](#)]
15. Zhang, H.; Zhang, J. A review of thermodynamic equilibrium and kinetic models for biosorption. *Tianzhong J.* **2009**, *24*, 19–22.
16. Wang, Y.; Zhou, M. Structure and adsorption properties of cotton-based activated carbon fibers. *Synth. Fiber Ind.* **2009**, *32*, 11–14.
17. Zhu, S.; Ye, Z.; Song, R.; He, D.; Gao, Y.; Li, J. Adsorption Behavior of Dendritic Hydrophobic Conjugated Polymers. *Fine Petrochem.* **2021**, *38*, 12–17.

Disclaimer/Publisher’s Note: The statements, opinions and data contained in all publications are solely those of the individual author(s) and contributor(s) and not of MDPI and/or the editor(s). MDPI and/or the editor(s) disclaim responsibility for any injury to people or property resulting from any ideas, methods, instructions or products referred to in the content.